ARTICLE
Journal of Cellular Biochemistry 115:1561–1571 (2014)

Journal of Cellular Biochemistry

Artificial Matrices With High-Sulfated Glycosaminoglycans and Collagen Are Anti-Inflammatory and Pro-Osteogenic for Human Mesenchymal Stromal Cells

Ute Hempel,[1]* Claudia Matthäus,[1] Carolin Preissler,[1] Stephanie Möller,[2] Vera Hintze,[3] and Peter Dieter[1]

[1]*Institute of Physiological Chemistry, Carl Gustav Carus Faculty of Medicine, TU Dresden, Fiedlerstrasse 42 D-01307, Dresden, Germany*

[2]*INNOVENT e. V., Biomaterials Department, Prüssingstrasse 27 B D-07745, Jena, Germany*

[3]*Max Bergmann Center of Biomaterials, Technical University Dresden, Budapester Straße 27 D-01069, Dresden, Germany*

ABSTRACT

Bone healing has been described to be most efficient if the early inflammatory phase is resolved timely. When the inflammation elevates or is permanently established, bone healing becomes impaired and, moreover, bone destruction often takes place. Systemic disorders such as diabetes and bone diseases like arthritis and osteoporosis are associated with sustained inflammation and delayed bone healing. One goal of biomaterial research is the development of materials/surface modifications which support the healing process by inhibiting the inflammatory bone erosion and suppressing pro-inflammatory mediators and by that promoting the bone repair process. In the present study, the influence of artificial extracellular matrices (aECM) on the interleukin (IL)-1β-induced pro-inflammatory response of human mesenchymal stromal cells (hMSC) was studied. hMSC cultured on aECM composed of collagen I and high-sulfated glycosaminoglycan (GAG) derivatives did not secrete IL-6, IL-8, monocyte chemoattractant protein-1, and prostaglandin E_2 in response to IL-1β. The activation and nuclear translocation of nuclear factor κBp65 induced by IL-1β, tumor necrosis factor-α or lipopolysaccharide was abrogated. Furthermore, these aECM promoted the osteogenic differentiation of hMSC as determined by an increased activity of tissue non-specific alkaline phosphatase (TNAP); however, the aECM had no effect on the IL-1β-induced TNAP activity. These data suggest that aECM with high-sulfated GAG derivatives suppress the formation of pro-inflammatory mediators and simultaneously promote the osteogenic differentiation of hMSC. Therefore, these aECM might offer an interesting approach as material/surface modification supporting the bone healing process. J. Cell. Biochem. 115: 1561–1571, 2014.

KEY WORDS: EXTRACELLULAR MATRIX; GLYCOSAMINOGLYCANS; INFLAMMATION; MESENCHYMAL STROMAL CELLS; OSTEOGENIC DIFFERENTIATION; PROSTAGLANDINS

Abbreviations: (a)ECM, (artificial) extracellular matrix; BM, basal medium; col, collagen; COX, cyclooxygenase; CS, chondroitin sulfate; DAPI, 4′,6-diamidino-2-phenylindole; Dex, dexamethasone; DKK-1, dickkopf-related protein-1; DMEM, Dulbecco's minimal essential medium; DS_S, degree of sulfation per disaccharide repeating unit; ELISA, enzyme-linked immunosorbent assay; ERK, extracellular-regulated kinase; GAG(s), glycosaminoglycan(s); HA, hyaluronan; hMSC, human mesenchymal stromal cells; IKK, IκB kinase; IL, interleukin; LPS, lipopolysaccharide; MCP-1, (CCL2) monocyte chemoattractant protein-1; MTS, (3-(4,5-dimethylthiazol-2-yl)-5-(3-carboxymethoxy-phenyl)-2-(4-sulfophenyl)-2H-tetrazolium); NFκB, nuclear factor κB; OM/D, osteogenic differentiation medium; PBS, phosphate-buffered saline; PGE_2, prostaglandin E_2; sCS3, high-sulfated CS (DS_S ~3); sHA3, high-sulfated hyaluronan (DS_S ~3); STAT, signal transducer and activator of transcription; TCPS, tissue culture polystyrene; TNAP, tissue non-specific alkaline phosphatase; TNF-α, tumor necrosis factor-α.

Current address of Claudia Matthäus is Max Delbrück Center for Molecular Medicine, Developmental Neurobiology, Robert-Rössle-Str. 10, 13092 Berlin, Germany.

*Correspondence to: Ute Hempel, Institute of Physiological Chemistry, Carl Gustav Carus Faculty of Medicine, Technische Universität Dresden, Fiedlerstrasse 42, D-01307 Dresden, Germany. E-mail: ute.hempel@tu-dresden.de

Manuscript Received: 23 January 2014; Manuscript Accepted: 4 April 2014

Accepted manuscript online in Wiley Online Library (wileyonlinelibrary.com): 7 April 2014

DOI 10.1002/jcb.24814 • © 2014 Wiley Periodicals, Inc.

Bone healing includes an inflammatory phase followed by bone formation and remodeling processes [Claes et al., 2012]. The inflammatory reaction is induced immediately after tissue damage by fracture, surgical intervention or by introducing an implant. Inflammatory cells such as granulocytes, monocytes and macrophages become activated and secrete various pro-inflammatory mediators which influence the differentiation/function of bone-forming osteoblasts, bone-resorbing osteoclasts and their mesenchymal and hematopoietic precursor cells. When exposed to an inflammatory environment, osteoblasts and mesenchymal stromal cells (MSC) themselves secrete various pro-inflammatory mediators and by that contribute to the sustainment of inflammation or to the repair process [Tomchuck et al., 2008]. A moderate, controlled and quickly resolved inflammatory reaction is essential for physiological bone healing; for example, anti-inflammatory drugs are known to have a negative effect on bone healing when they are applied in the early phase of inflammation [Pietrogrande et al., 2011]. Otherwise, the over-exposition of bones and joints with pro-inflammatory mediators, systemic and long-term chronic inflammation causes impaired or decelerated bone healing or even more bone/joint destructions as known from osteo- or rheumatoid arthritis [Blackwell et al., 2010; Bastian et al., 2011; Kapoor et al., 2011; Thomas and Puleo, 2011]. Yang et al. [2007] described a delayed bone healing in interleukin (IL)-6 knockout mice.

The switch from the positive effect of inflammation in early/initial bone healing to the negative effect of hyper-inflammation or chronic inflammation is associated with the number and subpopulation of inflammatory cells and secreted mediators [Bastian et al., 2011]. The release of pro-inflammatory mediators leads to the inhibition of osteoblast function partly by inhibition of the extracellular-regulated kinase (ERK1/2), activation of signal transducers and activators of transcription (STAT), activation of the nuclear factor (NF)κB, and up-regulation of the Dickkopf-related protein (DKK1) and sclerostin [Redlich and Smolen, 2012]. NFκB transcription factor is activated by a plethora of stimuli and mediates varied gene expression programs [Oeckinghaus et al., 2011]. Pro-inflammatory mediators such as IL-1β, tumor necrosis factor (TNF)-α and lipopolysaccharide (LPS), each interacting with its specific receptor, lead to the activation/phosphorylation of the IκB kinase (IKK) complex consisting of the catalytically active subunits IKKα, IKKβ, and the regulatory subunit IKKγ. The catalytically active IKK subunit phosphorylate IκB in the NFκB/IκB complex which results in release of the NFκB dimer from the complex, ubiquitinylation and proteasomal degradation of phospho-IκB, and translocation of NFκBp65/NFκBp50 heterodimer into the nucleus (canonical pathway) where it regulates the transcription of genes responsible for pro-inflammatory mediators [Ben-Neriah and Karin, 2011].

Glycosaminoglycans (GAGs) are multifunctional components of the pericellular and extracellular matrix (ECM). They consist of repeating disaccharide units, for example, of D-glucuronic acid-β(1→3)-*N*-acetyl-D-galactosamine-4-sulfate-β(1→4) (chondoitin sulfate) or of D-glucuronic acid-β(1→3)-*N*-acetyl-D-glucosamine-β(1→4) (hyaluronan). Sulfated negatively charged GAGs like chondroitin sulfate, dermatan sulfate or heparan sulfate are mostly covalently bound to core proteins forming proteoglycans which are part of membrane-spanning syndecans, GPI-anchored glypicans or associated to ECM as aggrecan, versican, biglycan, or decorin. The non-sulfated, negatively charged hyaluronan can form a backbone for several proteoglycans and is able to bind enormous amounts of water, to swell and function in several tissues as a space holder and immune modulator. GAGs interact with many cations and proteins and are able to modulate the bioavailability of growth factors, cytokines and chemokines [Macri et al., 2007]. GAGs act as co-receptors for many growth factors; for example, the association of basic fibroblast growth factor (bFGF) with heparan sulfate is important for the interaction of bFGF with its membrane receptor [Gallagher and Turnbull, 1992]. Natural sulfated glycosaminoglycans (GAGs), for example, chondroitin sulfate (CS), seem to have beneficial effects on the pathophysiology of osteoarthritis; they reduced blood markers of inflammation and the activity of destructive proteases like matrixmetalloproteinases, diminished pain and improved the function of the affected joint [Martell-Pelletier et al., 2010; Volpi, 2011; Hochberg et al., 2013].

Synthetically sulfated hyaluronan derivatives (sHA) were at first characterized and described as antithrombogenic substances [Magnani et al., 1996; Chen et al., 1997; Magnani et al., 1998] and inhibitors of TNF-α [Chang et al., 1994]. A pro-osteogenic effect of sulfated hyaluronan derivatives was described by Nagahata et al. [2004] with rat calvarial cells who demonstrated that the substances induced the formation of cell aggregates with increased activity of tissue non-specific alkaline phosphatase (TNAP). aECM composed of collagen (col) and synthetically high-sulfated GAG derivatives increased the osteogenic differentiation of hMSC [Hempel et al., 2012a]. These aECM are known to influence many cellular functions of hMSC such as cell–matrix interactions, signal transductions pathways and endocytosis [Büttner et al., 2013; Kliemt et al., 2013] and led to a considerable inhibition of osteoclast function [Salbach et al., 2012a].

In the present study, the influence of aECM containing col, the natural GAGs CS and HA as well as high-sulfated GAG derivatives on the response of hMSC to inflammatory stimuli was investigated. Particularly the effect on the formation of pro-inflammatory mediators [IL-6, IL-8, monocyte-chemoattractant protein-1 (MCP-1), and prostaglandin E_2 (PGE_2)] and the involvement of cyclooxygenase-2 (COX-2) and NFκB were analyzed. To examine the influence of aECM on the osteogenic differentiation of hMSC in response to IL-1β, the activity of TNAP was determined.

MATERIALS AND METHODS

Cell culture plastic material (TCPS) was from Greiner (Frickenhausen, Germany) and Nunc (Wiesbaden, Germany). Dulbecco's minimum essential medium (DMEM), trypsin, penicillin/streptomycin antibiotics, and phosphate buffered saline (PBS) were purchased from Biochrom (Berlin, Germany). Fetal calf serum was from BioWest (via Th.Geyer, Hamburg, Germany). LPS (*Salmonella minnesota*) and the other biochemical reagents were from Sigma (Taufkirchen, Germany). For the determination of protein concentration the RotiQuant assay from Roth (Karlsruhe, Germany) was used. For the determination of IL-1β, IL-6, IL-8, and MCP-1 concentration, DuoSet enzyme-linked immunosorbent assay (ELISA) Development Kits (R&D Systems, Wiesbaden, Germany) were used. For the determination of COX-2

protein, total COX-2 cell-based ELISA kit (R&D Systems) was used. The determination of NFκB activation was performed with the NFκBp65 TransAM™ Kit (Active Motif, La Hulpe, Belgium). Human IL-1β and hTNF-α were purchased from Peprotech (Hamburg, Germany). Rat tail collagen I was from BD Bioscience (Heidelberg, Germany). CS [from *bovine trachea*, mixture of CSA(70)/CSC(30)] was obtained from Sigma and HA (from *Streptococcus*) was obtained from Aqua Biochem (Dessau, Germany). High-sulfated chondroitin sulfate (sCS3, degree of sulfation per disaccharide (DS_S) ~3) derivative and high-sulfated hyaluronan (sHA3, $DS_S \sim 3$) derivative were synthesized as described earlier [Hempel et al., 2012b].

PREPARATION AND CHARACTERIZATION OF ARTIFICIAL EXTRACELLULAR MATRICES (aECM)

aECM were prepared from collagen I and CS, HA or the high sulfated GAG derivatives sCS3 and sHA3 and characterized as described earlier [Hempel et al., 2012a,b]. In brief, 1 mg collagen I was dissolved in 1 ml of ice cold 10 mM acetic acid and was mixed with an equal volume of 1 mg GAG derivative/ml dissolved in ice cold double concentrated fibrillogenesis buffer (50 mM sodium dihydrogenphosphate, 11 mM potassium dihydrogenphosphate, pH 7.4). Two hundred twenty microliters of the collagen I/sGAG derivative mixture per cm^2 were placed onto tissue culture polystyrene plates (TCPS). Fibrillogenesis was performed overnight at 37°C. The resulting aECM was air-dried, washed two times with 1 ml deionized, sterile water and air-dried again. Before the cell culture experiments, an additional washing step with sterile PBS for 1 h at 37°C was performed.

ISOLATION AND CULTIVATION OF HUMAN MESENCHYMAL STROMAL CELLS (hMSC)

The hMSC were isolated from bone marrow aspirates, obtained from Caucasian donors (average age 32 ± 7 years, mixed gender) at the Bone Marrow Transplantation Center of the University Hospital Dresden, and were characterized as described [Oswald et al., 2004]. The donors were informed about the procedures and gave their full consent. The study was approved by the local ethics commission (ethic vote No. EK114042009). Four hMSC preparations were chosen for the experiments according prior characterization of osteogenic differentiation capacity and according the characteristic: "similar basal TNAP activity in passage 1." hMSC preparations of individual donors were not pooled. The cells were used in passage 2–4. 7,000 hMSC/cm^2 were plated in Dulbecco's minimal essential medium (DMEM) with 10% heat-inactivated fetal calf serum and 10,000 IE penicillin/10,000 μg streptomycin/ml (=basal medium, BM) onto tissue culture polystyrene (TCPS) or aECM-coated TCPS.

For the determination of released pro-inflammatory mediators (IL-6, IL-8, MCP1, PGE_2), analysis of gene expression (*nfκB* and *cox-2*), COX-2 protein content and the MTS assay, sub-confluent hMSC (sub-confluence was seen 72 h after plating) were serum-starved in DMEM supplemented with 10,000 IE penicillin/10,000 μg streptomycin/ml for 24 h and treated afterwards with IL-1β (10 ng/ml) for 24 h. For the determination of NFκB activation, sub-confluent hMSC were serum-starved for 24 h and treated afterwards with IL-1β (10 ng/ml), TNF-α (10 ng/ml) or LPS (1 μg/ml), respectively, for 1 h.

For the determination of TNAP activity and mineral accumulation, hMSC were treated 24 h after plating in BM with 10 ng IL-1β/ml. At day 4 after plating, hMSC were cultured in BM or osteogenic differentiation medium (BM with 10 mM β-glycerophosphate, 300 μM ascorbic acid, 10 nM dexamethasone = OM/D); thereafter, the medium was changed twice per week and 10 ng IL-1β/ml was added with each medium change. At day 11 after plating, the activity of TNAP was determined. At day 22 after plating, the calcium phosphate deposition was quantified.

CONCENTRATION OF IL-6, IL-8, MCP-1, AND PGE_2

Twenty-four hours after IL-1β treatment, conditioned medium of hMSC was collected and analyzed for the concentration of IL-6, IL-8, and MCP-1 using DuoSet ELISA Development Kits according to manufacturer's instructions. PGE_2 concentration was determined with a competitive ELISA as described earlier [Dieter et al., 1999].

IL-1β RECOVERY

aECM were incubated with 10 ng IL-1β/ml in BM for 1 and 24 h at 37°C. The concentration of IL-1β in the conditioned medium was determined with human IL-1β DuoSet ELISA Development Kit according to manufacturer's instructions.

METABOLIC ACTIVITY

Metabolic activity of hMSC was determined by MTS assay (Cell Titer96 AQ_{ueous} One Solution Proliferation Assay) (Promega, Mannheim, Germany). For the analysis, conditioned medium was replaced by fresh medium containing 10% of MTS dye solution. After 2 h of incubation at 37°C in a humidified CO_2 incubator, 100 μl cellular medium was transferred into a 96-well plate and the absorbance of the formed MTS formazan dye was measured photometrically at 490 nm.

ACTIVATION, TRANSLOCATION, AND EXPRESSION OF NFκB

Activation: One hour after treatment with IL-1β, TNF-α, and LPS, hMSC were washed twice with PBS and lysed according to manufacturer's instructions for TransAM™ NFκBp65 assay. Protein concentration of the lysate was determined by Rotiquant® assay (Roth GmbH, Karlsruhe, Germany) and calculated from a linear calibration curve ($r = 0.9967$) obtained with bovine serum albumin. Four micrograms of cellular protein were applied to the TransAM™ NFκBp65 assay.

Translocation: For visualization of phospho-NFκB, hMSC were treated with IL-1β for 1 h, washed afterwards with PBS and fixed with 4% paraformaldehyde (w/v) in PBS for 10 min. After permeabilization with 0.1% Triton X-100 in PBS for 20 min, non-specific binding sites were blocked with 1% bovine serum albumin (w/v) in PBS containing 0.05% Tween-20. The cells were incubated for 1 h with rabbit-anti-human phospho-NFκBp65-Ser536 monoclonal antibody (Cell Signalling, Frankfurt a. M, Germany, no. #3031) dissolved in PBS, containing 1% bovine serum albumin and 0.05% Tween-20. After washing with PBS, cells were incubated with blocking buffer for 10 min again. AlexaFluor-568-conjugated goat-anti-rabbit polyclonal antibody (Invitrogen, Karlsruhe, Germany, no. A11011) dissolved in PBS containing 1% bovine serum albumin and 0.05% Tween-20, was used as a secondary antibody. Nuclei were stained with 0.2 μg 4′,6-diamidino-2-phenylindole (DAPI)/ml PBS for 10 min at 25°C. After staining, the cells were embedded in Mowiol

TABLE I. Primer Pairs Used for Real Time PCR

Gene	Accession no.	Forward primer	Reverse primer	Binding position	Product length (bp)	Product identity (%)[a]
actin[b]	NM001101.3	aatgtggccgaggactttgattgc	ttaggatggcaagggacttcctgt	1,414–1,508	95	100
gapdh[b]	NM002046.3	tgttcgtcatgggtgtgaacca	tgatggcatggactgtggtcat	563–718	156	97
nfκB[b]	NM003998.3	accctgaccttgcctatttg	agctctttttcccgatctcc	985–1,054	70	100
cox-2[b]	NM000963.1	caaatccttgctgttcccaccca	tgcactgtgtttggagtgggtttc	187–358	172	98

[a]Determined by sequencing of amplified DNA products.
[b]Genes: *actin*, β-actin; *gapdh*, glyceraldhehyde-3-phosphate dehydrogenase; *nfκb*, nuclear factor κB; *cox-2*, cyclooxygenase-2.

4-88 (Sigma) and visualized using an AxioPhot fluorescence microscope (Carl Zeiss, Oberkochen, Germany). The fluorescence signals were detected using the following filters: excitation 546 nm and emission 590 nm for AlexaFluor-568 and excitation 365 nm and emission 420 nm for DAPI. Digital images were obtained with an AxioCam MRm camera (Carl Zeiss) by using AxioVision software release 4.6 (Carl Zeiss).

Gene expression: For the analysis of *nfκB* gene expression, RNA was prepared from cell lysates after 24 h of treatment with IL-1β using RNeasy Mini Kit (Qiagen, Hilden Germany). cDNA was synthesized using the QuantiTect Reverse Transcription Kit (Qiagen) including a DNA digestion step. Real-time PCR reactions were performed using RotorGene PG-3000 PCR machine (Corbett, Wasserburg, Germany) with the RotorGene SYBR Green PCR Kit (Qiagen). After the initial activation step at 95°C for 5 min, 50 PCR cycles (denaturation at 95°C for 5 s; annealing and synthesis at 60°C for 10 s) were carried out. Primers were constructed by use of Universal Probe Library (Roche, Mannheim Germany) (see Table I for detailed information) and synthesized by Eurofines MWG Operon (Ebersberg, Germany). The same single stranded cDNA was used to analyze the expression of the gene of interest and the house-keeping genes *beta-actin* and *gapdh*. The relative expression values were calculated with both *beta-actin* and *gapdh* using the comparative quantification method of the RotorGene software release 6.0. The values are normalized to hMSC in BM on TCPS.

COX-2 GENE EXPRESSION AND PROTEIN

Gene expression of *cox-2* was analyzed as described above (see Table I for detailed information). COX-2 protein content was quantified with the total COX-2 cell-based ELISA kit (KCB4198; R&D systems) according to manufacturer's instructions. The fluorescence signal was determined using a fluorescence plate reader (FluoroStar Optima, BMG Labtech, Ortenberg, Germany) with excitation at 540 nm and emission at 600 nm for COX-2 and with excitation at 360 nm and emission at 450 nm for GAPDH. COX-2 amount was normalized to GAPDH amount.

TNAP ACTIVITY

TNAP activity was determined in cell lysates (lysis buffer: 1.5 M Tris–HCl (pH 10), 1 mM $ZnCl_2$, 1 mM $MgCl_2$ and 1% Triton X-100) with *p*-nitrophenylphosphate as a substrate as described previously [Hempel et al., 2012a] and calculated from a linear calibration curve ($r = 0.9979$) prepared with *p*-nitrophenol. Specific TNAP activity is given in mU/mg protein. Protein concentration of the lysate was determined as described above.

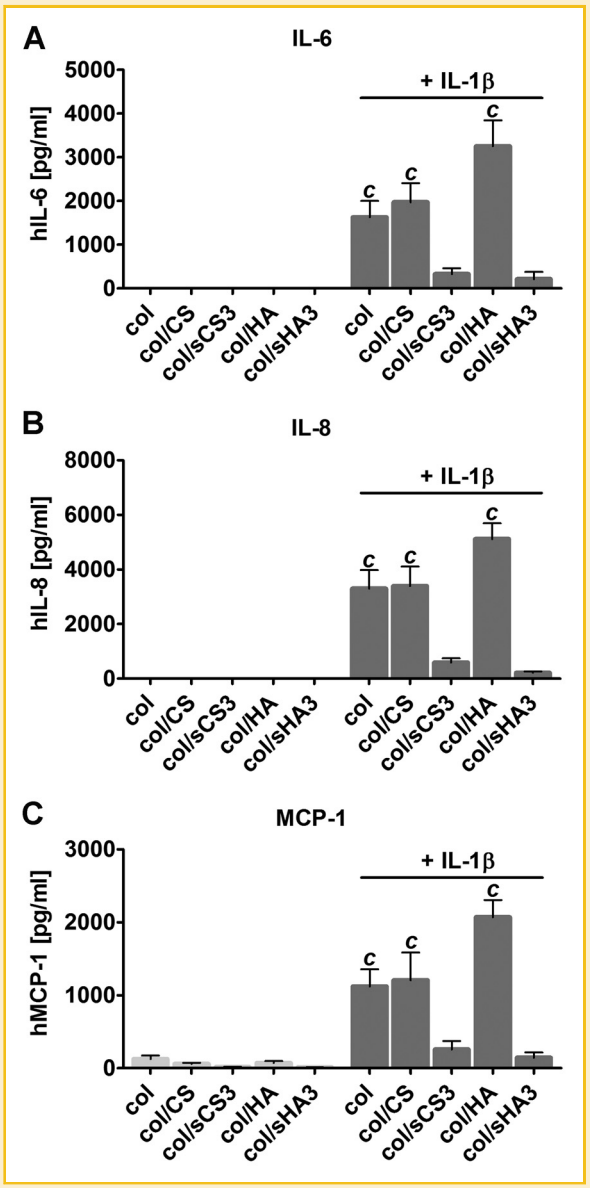

Fig. 1. Formation of IL-6, IL-8, and MCP-1. hMSC (7,000 cells/cm^2) were cultured on aECM composed of collagen and CS, sCS3, HA, and sHA3 in BM. At day 3 after plating, hMSC were serum-starved for 24 h. Then the cells were treated with 10 ng IL-1β/ml for 24 h. The concentration of IL-6 (A), IL-8 (B), and MCP-1 (C) was determined in conditioned medium by ELISA. The data are presented as mean ± SEM, n = 4. Significant differences of IL-1β treatment versus untreated cells comparing the same aECM were indicated as *c* ($P < 0.001$).

CALCIUM PHOSPHATE DEPOSITION

Calcium phosphate deposition was quantified with the calcium and the phosphorus kit (both from Greiner Diagnostics, Bahlingen, Germany) as previously described [Hempel et al., 2012a]. Cell layers were washed with PBS, dried and incubated with 0.5 M HCl at 4°C for 24 h. Calcium and phosphate content in the lysates were quantified photometrically with cresolphthalein complexone at 570 nm and ammonium molybdate at 340 nm, respectively. Both, calcium and phosphate content (μmol/cm^2) was calculated from linear calibration curves ($r > 0.99$). Cell-free aECM samples (control) were treated in the same way as aECM with cultured cells and analyzed for calcium and phosphate.

STATISTICAL ANALYSIS

The experiments were performed with hMSC from four different donors, each in triplicate. The results are presented as mean ± standard error of the mean (SEM). Statistical significance was analyzed with GraphPad Prism 5.04 software (Statcon, Witzenhausen, Germany) by two-way ANOVA analysis with Bonferroni's post-test. Significant differences of IL-1β treated cells versus untreated cells comparing the same aECM were indicated with italic characters (*a* for $P < 0.05$, and *c* for $P < 0.001$). Significant differences of GAG-aECM versus col were indicated by hash mark (# for $P < 0.001$).

RESULTS

For all in vitro experiments, MSC were cultured onto five different aECM. To evaluate directly the effect of IL-1β, TNF-α, and LPS on NFκB activation, serum-starved hMSC were treated for 1 h with these stimuli (pre-tests showed maximum NFκB activation at this time point). To evaluate directly the effect of IL-1β on the formation of IL-6, IL-8, MCP-1, and PGE_2 as well as on expression and protein level of COX-2, and on expression of *nfκb*, serum-starved hMSC were treated for 24 h (pre-tests showed maxima for these parameters). To evaluate the effect of IL-1β on osteogenic differentiation, hMSC were cultured either in BM or in OM/D until day 11 (early differentiation phase indicated by increasing TNAP activity) and day 22 (late differentiation phase indicated by increasing calcium phosphate accumulation) with permanent addition of IL-1β.

INFLUENCE OF aECM AND IL-1β ON THE FORMATION OF IL-6, IL-8, AND MCP-1

hMSC which were cultured on different aECM, treated with IL-1β for 24 h and analyzed for the formation of IL-6 (Fig. 1A), IL-8 (Fig. 1B), and MCP-1 (Fig. 1C). Untreated cells showed no or only a marginal release of IL-6, IL-8, and MCP-1 on all aECM. IL-1β induced a strong significant ($P < 0.001$) increase of IL-6, IL-8, and MCP-1 in hMSC on col, col/CS, and col/HA; in contrast, only a weak not significant formation of IL-6, IL-8, and MCP-1 was induced in hMSC cultured on the high-sulfated aECM col/sCS3 and col/sHA3.

To exclude that the aECM or treatment with IL-1β had an effect on the metabolic activity of the cells, the MTS assay was performed. The metabolic activity of cells was neither affected by the aECM or the addition of IL-1β (Fig. 2A). To exclude that IL-1β was trapped by the aECM with high-sulfated GAG derivatives, the recovery of IL-1β after 1 and 24 h of incubation with the aECM at 37°C was analyzed. After 1 h 96.7 ± 1.8% and after 24 h 90.9 ± 1.4% of the added IL-1β was found in the conditioned medium independently on the aECM (Fig. 2B) indicating that all aECM did not markedly bind IL-1β.

INFLUENCE OF aECM AND IL-1β ON THE ACTIVATION, GENE EXPRESSION, AND TRANSLOCATION OF NFκB

The transcription factor NFκB is activated in response to inflammatory stimuli and regulates the formation of certain pro-inflammatory mediators such as IL-6, IL-8, and MCP-1 [Novack, 2011]. For the analysis of NFκB activation an ELISA for measurement of NFκBp65-binding to its consensus DNA site was used. Untreated cells showed on all aECM a marginal and comparable activation of NFκBp65. IL-1β, TNF-α and LPS induced an about 5–10-fold significant ($P < 0.001$) activation of NFκBp65 in hMSC on col, col/CS, and col/HA but only a small not significant activation on the high-sulfated aECM col/sCS3 and col/sHA3

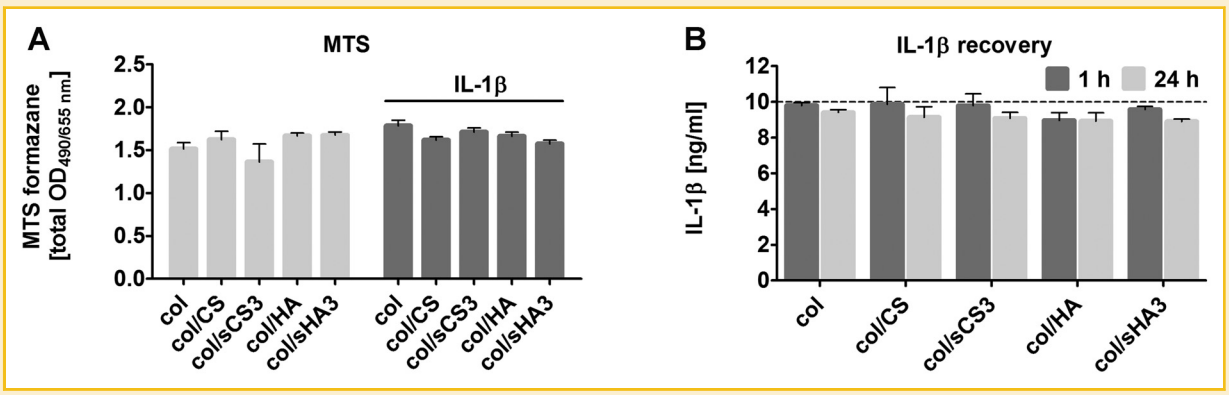

Fig. 2. Metabolic activity and IL-1β recovery. hMSC (7,000 cells/cm^2) were cultured on aECM composed of collagen and CS, sCS3, HA, and sHA3. At day 3 after plating, hMSC were serum-starved for 24 h. Then the cells were treated with 10 ng IL-1β/ml for 24 h. The metabolic activity was measured by MTS assay (A). Data presented as mean ± SEM, n = 4. B: aECM were incubated at 37°C for 1 and 24 h with 10 ng IL-1β/ml in BM. IL-1β concentration in conditioned medium was determined by ELISA. The recovery of IL-1β is shown; the dotted line represents the initial IL-1β concentration, n = 3.

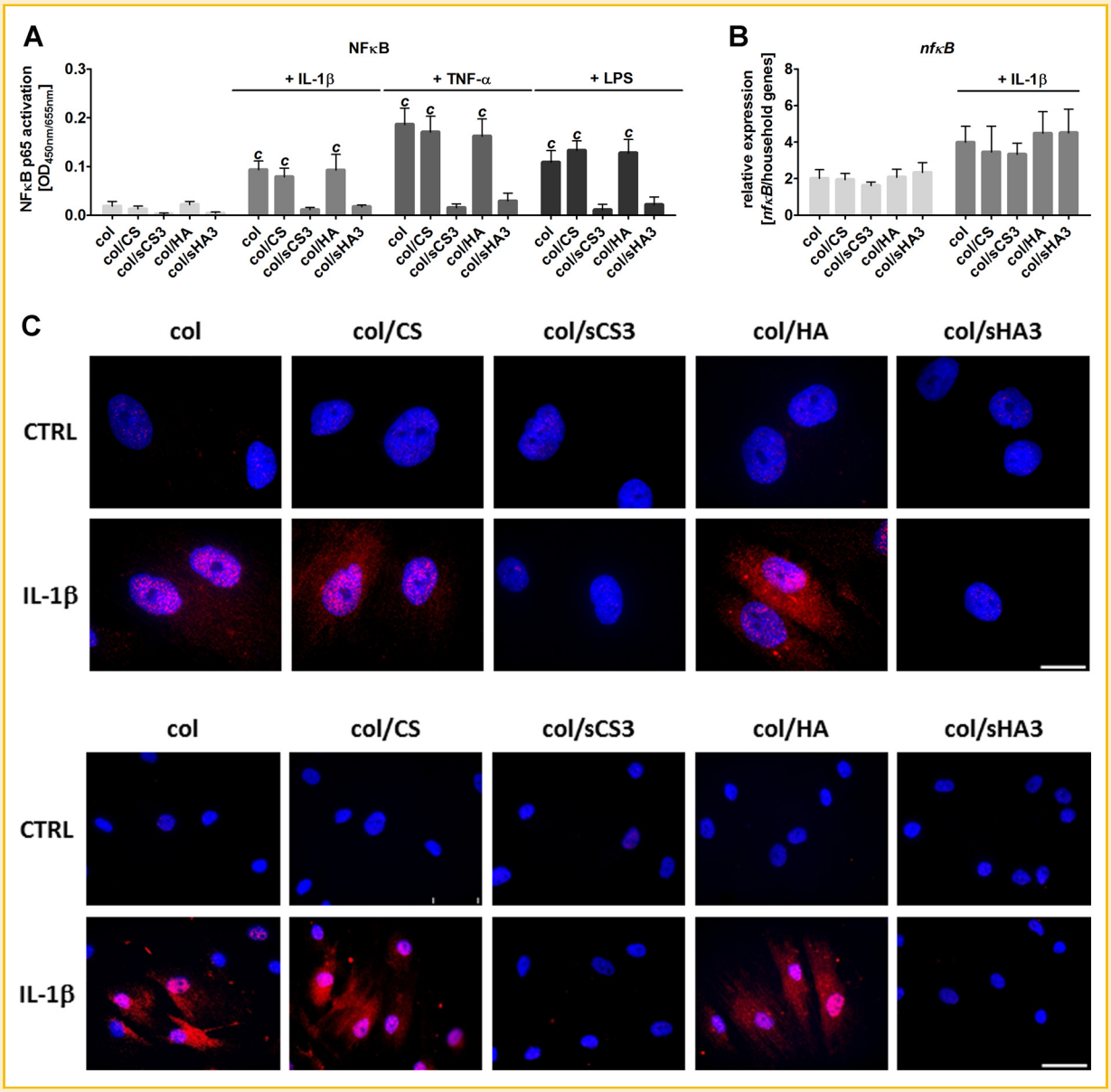

Fig. 3. Activation, expression, and translocalization of NFκB. hMSC (7,000 cells/cm^2) were cultured on aECM composed of collagen and CS, sCS3, HA, and sHA3 in BM. At day 3 after plating, hMSC were serum-starved for 24 h. A: Activation: hMSC were treated with 10 ng IL-1β/ml, 10 ng TNF-α/ml and 1 μg LPS/ml for 1 h and analyzed for NFκB DNA-binding activity using the TransAM™ NFκBp65 assay. Data presented as mean ± SEM, n = 4. Significant differences of treated cells versus untreated cells comparing the same aECM were indicated as c ($P < 0.001$). B: Gene expression: hMSC were treated with 10 ng IL-1β/ml for 24 h. The expression of *nfκB* was assessed by real time PCR and is related to expression of *beta-actin* and *gapdh*. The data are presented as mean ± SEM, n = 4. C: Translocation: hMSC were treated with 10 ng IL-1β/ml for 1 h and analyzed for phospho-NFκBp65-Ser-536. hMSC were fixed and stained with rabbit anti-phospho-NFκBp65-Ser536-monoclonal antibody/AlexaFluor-568 anti-rabbit IgG (red fluorescence) and DAPI for nuclei (blue fluorescence). Typical images are shown; scale bar = 50 μm.

(Fig. 3A). The aECM had no effect on the basal or IL-1β-induced expression of *nfκB* (Fig. 3B). IL-1β increased slightly but not significantly the expression of *nfκB*.

IL-1β induces the phosphorylation and translocation of NFκBp65 into the nucleus [Perkins, 2006]. Here, similar results were found for IL-1β stimulated hMSC on col, col/CS, and col/HA where phospho-NFκBp65-Ser536 was found cytosolic and co-localized with the nucleus; however, in hMSC on the high-sulfated col/sCS3 and col/sHA3 no phospho-NFκBp65-Ser536 could be detected after IL-1β treatment (Fig. 3C).

INFLUENCE OF aECM AND IL-1β ON THE COX-2 GENE EXPRESSION, COX-2 PROTEIN, AND PGE_2 FORMATION

NFκB is involved in the IL-1β-induced expression of COX-2 and the COX-2 mediated formation of PGE_2 [Nakao et al., 2002; Hirata et al., 2009]. IL-1β induced a significant ($P < 0.001$) expression of

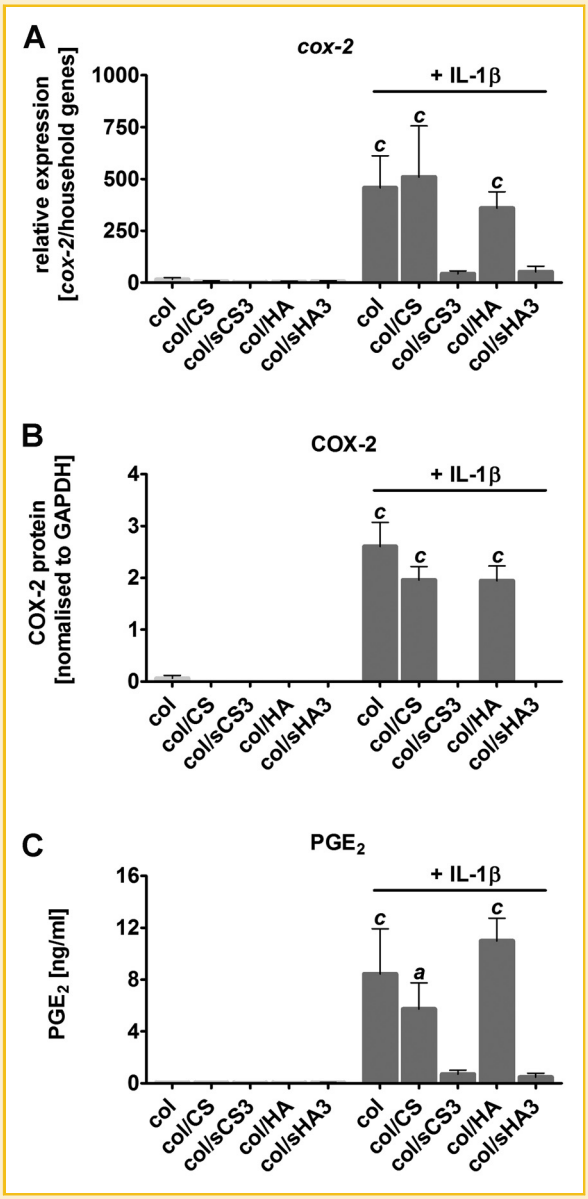

Fig. 4. Expression of COX-2 and PGE_2 formation. hMSC (7,000 cells/cm^2) were cultured on aECM composed of collagen and CS, sCS3, HA, and sHA3 in BM. At day 3 after plating, hMSC were serum-starved for 24 h. A: Gene expression: Cells were treated with 10 ng IL-1β/ml for 24 h. The expression of *cox-2* was assessed by real time PCR and is related to expression of *beta-actin* and *gapdh*. B: COX-2 protein content: The amount of COX-2 protein was assessed by total COX-2 cell-based ELISA kit and related to GAPDH protein content in the same cell lysate. C: PGE_2 formation: PGE_2 concentration in the conditioned medium was determined by ELISA (C). The data are presented as mean ± SEM, n = 4. Significant differences of IL-1β treatment versus untreated cells comparing the same aECM were indicated as *a* ($P < 0.05$) and *c* ($P < 0.001$).

cox-2 (Fig. 4A), a significant ($P < 0.001$) increase of COX-2 protein (Fig. 4B) and in consequence a significant ($P < 0.001$ for col and col/HA; $P < 0.05$ for col/CS) formation of PGE_2 (Fig. 4C) in hMSC on col, col/CS, and col/HA whereas no or only a marginal response could be measured in hMSC on the high-sulfated col/sCS3 and col/sHA3.

INFLUENCE OF aECM AND IL-1β ON TNAP ACTIVITY AND CALCIUM PHOSPHATE DEPOSITION

An increase of the TNAP activity is often used as a marker for osteogenic differentiation of MSC [Pittenger, 2008]. Here, hMSC in BM (undifferentiated cells, Fig. 5A) or OM/D (differentiated cells, Fig. 5B) showed at day 11 after plating a significant ($P < 0.001$) two- to threefold increase of TNAP activity on the high-sulfated col/sCS3 and col/sHA3 compared to the other aECM. IL-1β induced an increased TNAP activity in hMSC in BM and OM/D on col, col/CS, and col/HA but did not increase TNAP activity in cells on col/sCS3 and col/sHA3 (Fig. 5A,B). Calcium phosphate deposition around the cells requires TNAP activity; the enzyme releases phosphate from the in vitro substrate β-glycerophosphate which lead to calcium phosphate deposition afterwards. Although hMSC in BM revealed TNAP activity, they did not deposit calcium phosphate because of the lack of β-glycerophosphate in the medium. At day 22 after plating, calcium phosphate deposition was seen in differentiated hMSC in OM/D with a significant ($P < 0.001$) increase of calcium (Fig. 6A) and phosphate (Fig. 6B) on the high-sulfated col/sCS3 and col/sHA3 compared to the other aECM. IL-1β induced an increased calcium phosphate deposition in OM/D on col, col/CS, and col/HA but not on col/sCS3 and col/sHA3. These data are in line with results of TNAP activity. By plotting TNAP activity at day 11 versus calcium (Fig. 6C) and phosphate (Fig. 6D) at day 22, respectively, a linear correlation was seen. The ratio of the slopes, 5.513 ± 0.0906 for calcium (Fig. 6C) and 3.396 ± 0.0576 for phosphate (Fig. 6D), reflects the calcium to phosphate ratio and was with a value of 1.62 only slightly below the calcium to phosphate ratio in hydroxyapatite (1.67).

DISCUSSION

Recently we showed that aECM composed of collagen and over-sulfated GAG derivatives had a pro-osteogenic effect on hMSC [Hempel et al., 2012a]. The present study focuses on the influence of those aECM on the IL-1β-induced inflammatory response of hMSC. The exposure of hMSC to an inflammatory environment might affect the osteogenic differentiation process of the cells and results in a subsequent impaired bone formation and bone healing processes [Bastian et al., 2011; Thomas and Puleo, 2011; Kapoor et al., 2011]. Here we demonstrated that aECM containing high-sulfated GAG derivatives were able to suppress IL-1β-induced pro-inflammatory responses of hMSC but enhanced simultaneously the osteogenic differentiation of the cells. aECM containing high-sulfated HA and CS derivatives inhibited the IL-1β-induced formation of IL-6, IL-8, and MCP-1. The aECM also suppressed the expression of *cox-2*, the amount of COX-2 protein and the formation of PGE_2. Furthermore, the osteogenic differentiation of hMSC, as determined by the osteogenic marker TNAP and calcium phosphate deposition was enhanced by these aECM.

The inflammatory mediator IL-1β exerts its effects preferentially via activation and nuclear translocation of NFκB and also via activation of ERK1/2 and MAPK p38 [Oeckinghaus et al., 2011; Novack, 2011]; phosphorylated NFκBp65-Ser536, for example, has been shown to be essential for IL-1β induced IL-8 formation [Buss et al., 2004]. NFκB is discussed as a negative regulator of osteoblast

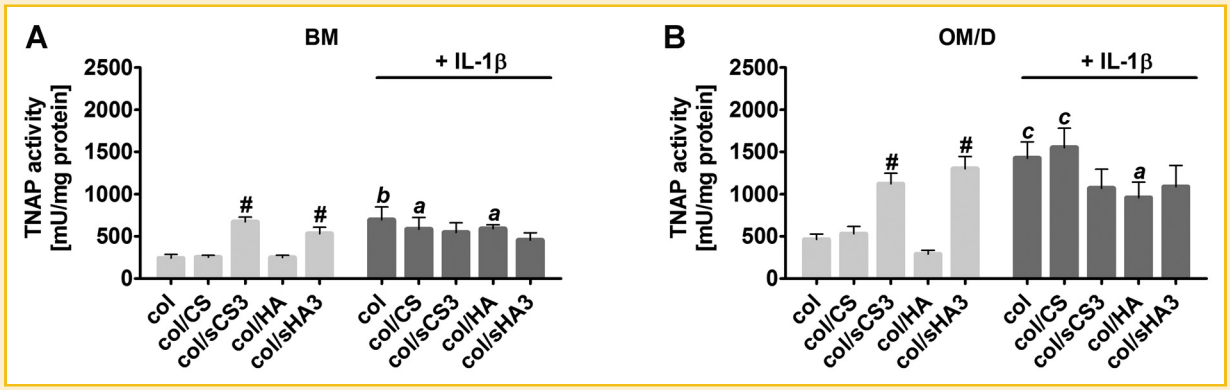

Fig. 5. Activity of TNAP. hMSC (7,000 cells/cm^2) were cultured on aECM composed of collagen and CS, sCS3, HA, and sHA3 in BM. Twenty-four hours after plating hMSC were treated with 10 ng IL-1β/ml. From day 4 after plating, hMSC were either incubated in BM (A) or OM/D (B). The data are presented as mean ± SEM, n = 4. Significant differences of IL-1β treatment versus untreated cells comparing the same aECM were indicated as *a* ($P < 0.05$) and *c* ($P < 0.001$). Significant differences of GAG-aECM versus col were indicated as # ($P < 0.001$).

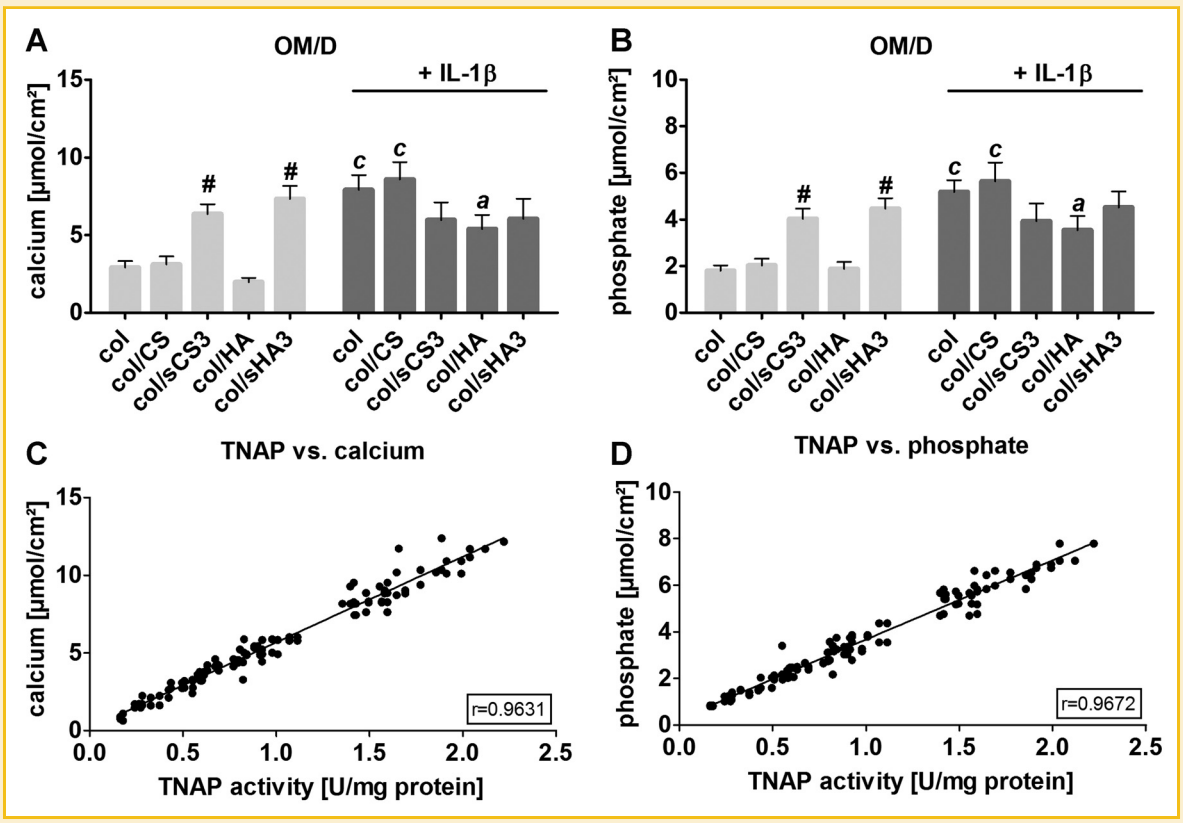

Fig. 6. Calcium phosphate deposition. hMSC (7,000 cells/cm^2) were cultured on aECM composed of collagen and CS, sCS3, HA, and sHA3 in BM. Twenty-four hours after plating hMSC were treated with 10 ng IL-1β/ml. From day 4 after plating, hMSC were incubated BM or OM/D. At day 22 after plating, calcium and phosphate deposition by hMSC was determined complexometrically. The amount of calcium (A) and phosphate (B) deposited by hMSC in OM/D are presented as mean ± SEM, n = 4. Significant differences of IL-1β treatment versus untreated cells comparing the same aECM were indicated as *a* ($P < 0.05$) and *c* ($P < 0.001$). Significant differences of GAG-aECM versus col were indicated as # ($P < 0.001$). The values of TNAP activity at day 11 in OM/D were plotted against the corresponding calcium (C) and phosphate (D) values at day 22. The linear equation for TNAP versus calcium was $y = (5.513 \pm 0.091)x + 0.1678 \pm 0.1014$ (C) and for TNAP versus phosphate $y = (3.396 \pm 0.0576)x + 0.2769 \pm 0.0647$ (D); the correlation coefficients r are given in the plots.

differentiation [Novack, 2011]. An up-regulation of NFκB has been implicated in the pathogenesis of several inflammation-related bone diseases including osteoporosis, osteo- and rheumatic arthritis [Krum et al., 2010]. Chang et al. [2009] showed that activation of NFκB by pro-inflammatory mediators suppresses the expression of Fos-related antigen-1 which is important for bone formation and bone matrix deposition and that the inhibition of IKK/NFκB pathway in differentiating osteoblasts can prevent osteoporotic bone loss. Here we showed that IL-1β induced the activation and translocation of NFκB only in hMSC which were cultured on aECM containing col, col/CS, and col/HA. In hMSC which were cultured on aECM containing high-sulfated GAG derivatives, IL-1β did not lead to an activation of NFκB; moreover, these effect was independent of the stimulus and almost identical for stimulation with IL-1β, TNF-α, and LPS suggesting that the high-sulfated GAGs could directly interact with the activation and translocation process of NFκB. A recent study with macrophages demonstrated that such aECM with col and high-sulfated HA suppressed the activity of pro-inflammatory macrophages by abrogating NFκB activation indicating that the effect of these aECM is not only restricted to hMSC [Franz et al., 2013]. In several models of induced inflammation, natural chondroitin sulfate was reported to inhibit NFκB activation [Cañas et al., 2010]. Campo et al. [2008, 2009] showed that chondroitin sulfate prevents NFκB translocation in response to LPS and interferes with the NFκB activation pathway at the level of LPS receptor TLR-4. However, in rat calvarial osteoblasts [Kunze et al., 2010] and, as seen here in hMSC, chondroitin sulfate had no effect on the IL-1β-induced NFκB translocation.

PGE_2 has also been shown to be elevated in an inflammatory environment via NFκB-induced COX-2 [Nakao et al., 2002; Hirata et al., 2009]. The role of PGE_2 in bone formation/bone remodeling is ambiguous described: COX-2/PGE_2 are important for bone formation associated with bone healing, but are also associated with enhanced bone resorption induced by inflammation [Blackwell et al., 2010]. Chondroitin sulfate has been described to have a protective effect on osteoarthritis probably by inhibition of PGE_2 formation [Pecchi et al., 2012]. The high-sulfated GAG heparin as a modification of titanium-based biomaterials promoted the function of MG-63 osteoblast cell line and inhibited their inflammation response [Kim et al., 2011].

Although pro-inflammatory mediators lead to bone loss in many inflammation-associated diseases such as rheumatoid arthritis, osteoporosis, and diabetes, they are known to promote ectopic bone formation and calcification, for example, of the endothelium [Ding et al., 2009]. Therefore it was assumed that the induction of osteogenesis in response to inflammation could be an important prerequisite for bone healing and remodeling and also the reason of the excessive ossification as known from the inflammatory bone disease ankylosing spondylitis [Scotti et al., 2013]. Ding et al. [2009] demonstrated that IL-1β and TNF-α increased TNAP activity and calcium phosphate accumulation in vitro. TNF-a-induced osteogenic differentiation of hMSC, for example, involves the osteogenesis regulating mediators Wnt5a and Wnt10b [Lin et al., 2010; Briolay et al., 2013]. The effects of IL-1β were strongly dependent on the duration and the time point of exposition as well as on the differentiation status of the cells: when premature MSC were exposed for a short time to IL-1β, an enhanced osteogenic differentiation was seen; in contrast, when osteoblasts received a long-term IL-1β-treatment, bone formation was rather inadequate [Lin et al., 2010]. Mumme et al. [2012] showed that IL-1β revealed its pro-inflammatory effect via NFκB whereas ERK1/2 was involved in the pro-osteogenic effect of IL-1β. The inhibition of NFκB promoted TNAP activity, expression of c*ol(1)α1*, *osteocalcin*, and *osteopontin* in mesenchymal cells [Krum et al., 2010]. An enhanced osteogenic differentiation in periodontal ligament-derived MSC after inhibition of NFκB was described and explained by competition of NFκB-signaling with Wnt/β-catenin signaling [Chen et al., 2013].

It is described that sulfated GAGs act as important co-regulators of hMSC lineage commitment, osteoprogenitor cell fate and bone formation and exert their effects often by interaction with bone-related growth factors whose activity can be reduced or enhanced thereby [Macri et al., 2007]. The regenerative potential of several GAGs has been well described [Salbach et al., 2012b]. Recent studies provided evidence that synthetically over-sulfated GAG derivatives, containing additional sulfate groups per disaccharide repeating unit, enhanced osteogenic differentiation of hMSC as determined by an induction of TNAP and an enhancement of calcium phosphate deposition probably in a growth factor (e.g., bone morphogenetic protein)- and dexamethasone-independent manner [Hempel et al., 2012a; Büttner et al., 2013].

To summarize, the anti-inflammatory but pro-osteogenic reactions of hMSC cultured on aECM with high-sulfated GAG derivatives were probably induced by a suppression of the activation of NFκB mediated by high-sulfated GAG derivatives. Therefore, all downstream events such as nuclear translocation of NFκB and expression of pro-inflammatory mediators and *cox-2* were found to be abrogated. Whether the effects of the high-sulfated GAG derivatives were due to upstream-processes of the NFκB activation cascade (suggesting an intracellular mechanism) or to an interference with cell receptors (suggesting an extracellular mechanism) remain to be elucidated. In conclusion, synthetically over-sulfated GAG derivatives in combination with collagen I facilitate anti-inflammatory but pro-osteogenic reactions of hMSC and might be appropriate for tissue engineering approaches and biomaterial modifications.

ACKNOWLEDGMENTS

The authors are very grateful to Professor Bornhäuser and colleagues from the stem cell lab of the University Hospital in Dresden for providing the human mesenchymal stromal cells. This work was supported by grant of Deutsche Forschungsgemeinschaft (SFB/TR67 projects B1, A2, and A3).

REFERENCES

Bastian O, Pillay J, Alblas J, Leenen L, Koenderman L, Blokhuis T. 2011. Systemic inflammation and fracture healing. J Leukoc Biol 89:669–673.

Ben-Neriah Y, Karin M. 2011. Inflammation meets cancer, with NFκB as the matchmaker. Nat Immunol 12:715–723.

Blackwell KA, Raisz LG, Pilbeam CC. 2010. Prostaglandins in bone: Bad cop, good cop?. Trends Endocrinol Metab 21:294–301.

Briolay A, Lencel P, Bessueille L, Caverzasio J, Buchet R, Magne D. 2013. Autocrine stimulation of osteoblast activity by Wnt5a in response to TNF-α in human mesenchymal stromal cells. Biochem Biophys Res Commun 430: 1072–1077.

Buss H, Dörrie A, Schmitz ML, Hoffmann E, Resch K, Kracht M. 2004. Constitutive and interleukin-1-inducible phosphorylation of p65 NF-öB at serine 536 is mediated by multiple protein kinases including IöB kinase (IKK)κ, IKKα, IKKβ, TRAF family member-associated (TANK)-binding kinase 1 (TBK1), and an unknown kinase and couples p65 to TATA-binding protein-associated factor II31-mediated interleukin-8 transcription. J Biol Chem 279:55633–55643.

Büttner M, Möller S, Keller M, Huster D, Schiller J, Schnabelrauch M, Dieter P, Hempel U. 2013. Over-sulfated chondroitin sulfate derivatives induce osteogenic differentiation of human mesenchymal stromal cells independent of bone morphogenetic protein-2 and transforming growth factor-ü1 signalling. J Cell Physiol 228:330–340.

Campo GM, Avenoso A, Campo S, D'Ascola A, Traina P, Calatroni A. 2008. Chondroitin-4-sulphate inhibits NF-'B translocation and caspase activation in collagen-induced arthritis in mice. Osteoarthritis Cartilage 16:1474–1483.

Campo GM, Avenoso A, Campo S, Traina P, D'Ascola A, Calatroni A. 2009. Glycosaminoglycans reduced inflammatory response by modulating toll-like receptor-4 in LPS-stimulated chondrocytes. Arch Biochem Biophys 491:7–15.

Cañas N, Gorina R, Planas AM, Vegés J, Montell E, García AG, López MG. 2010. Chondroitin sulfate inhibits lipopolysaccharide-induced inflammation in rat astrocytes by preventing nuclear factor kappa B activation. Neuroscience 167:872–879.

Chang NS, Intieri C, Mattison J, Armand G. 1994. Synthetic polysulfated hyaluronic acid is a potent inhibitor for tumor necrosis factor production. J Leukoc Biol 55:778–784.

Chang J, Wang Z, Tang E, Fan Z, McCauley L, Franceschi R, Guan K, Krebsbach PH, Wang CY. 2009. Inhibition of osteoblastic bone formation by nuclear factor-kappaB. Nat Med 15:682–689.

Chen G, Ito Y, Imanishi Y, Magnani A, Lamponi S, Barbucci R. 1997. Photoimmobilization of sulfated hyaluronic acid for antithrombogenicity. Bioconj Chem 8:730–734.

Chen X, Hu C, Wang LL, Kong X, Ding Y, Jin Y. 2013. Nuclear factor-κB modulates osteogenesis of periodontal ligament stem cells through competition with β-catenin signaling in inflammatory microenvironments. Cell Death Dis 4:e510. DOI: 10.1038/cddis.2013.14

Claes L, Recknagel S, Ignatius A. 2012. Fracture healing under healthy and inflammatory conditions. Nat Rev Rheumatol 8:133–143.

Dieter P, Hempel U, Kamionka S, Kolada A, Malessa B, Fitzke E, Tran-Thi TA. 1999. Prostaglandin E2 affects differently the release of inflammatory mediators from resident macrophages by LPS and muramyl tripeptides. Mediat Inflamm 8:295–303.

Ding J, Ghali O, Lencel P, Broux O, Chauveau C, Devedjian JC, Hardouin P, Magne D. 2009. TNF-α and IL-1 inhibit RUNX2 and collagen expression but increase alkaline phosphatase activity and mineralization in human mesenchymal stem cells. Life Sci 84:499–504.

Franz S, Allenstein F, Kajahn J, Fortsreuter I, Hintze V, Möller S, Simon JC. 2013. Artificial extracellular matrices composed of collagen I and high-sulfated hyaluronan promote phenotype and functional modulation of human pro-inflammatory M1 macrophages. Acta Biomater 9:5621–5629.

Gallagher JT, Turnbull JE. 1992. Heparan sulphate in the binding and activation of basic fibroblast growth factor. Glycobiology 2:523–528.

Hempel U, Hintze V, Möller S, Schnabelrauch M, Scharnweber D, Dieter P. 2012a. Artificial extracellular matrices composed of collagen I and sulfated hyaluronan with adsorbed transforming growth factor ö1 promote collagen synthesis of human mesenchymal stromal cells. Acta Biomater 8:659–666.

Hempel U, Möller S, Noack C, Hintze V, Scharnweber D, Schnabelrauch M, Dieter P. 2012b. Sulfated hyaluronan/collagen I-matrices enhance osteogenic differentiation of human mesenchymal stromal cells in vitro even in the absence of dexamethasone. Acta Biomater 8:4064–4072.

Hirata M, Kobayashi M, Takita M, Masumoto C, Miyaura C, Inada M. 2009. Hyaluronan inhibits bone resorption by suppressing prostaglandine E synthesis in osteoblasts treated with interleukin-1. Biochem Biophys Res Commun 381:139–143.

Hochberg M, Chevalier X, Henrotin Y, Hunter DJ, Uebelhart D. 2013. Symptom and structure modification in osteoarthritis with pharmaceutical-grade chondroitin sulfate: What's the evidence?. Curr Med Res Opin 29: 259–267.

Kapoor M, Martel-Pelletier J, Lajeunesse D, Pelletier J-P, Fahmi H. 2011. Role of pro-inflammatory cytokines in the pathophysiology of osteoarthritis. Nature Rev Rheumatol 7:33–42.

Kim SE, Song SH, Yun YP, Choi BJ, Kwon IK, Bae MS, Moon HJ, Kwon YD. 2011. The effect of immobilization of heparin and bone morphogenetic protein-2 (BMP-2) to titanium surfaces on inflammation and osteoblast function. Biomaterials 32:366–373.

Kliemt S, Lange C, Otto W, Hintze V, Möller S, von Bergen M, Hempel U, Kalkhof S. 2013. Sulfated hyaluronan containing collagen matrices enhance cell-matrix-interaction, endocytosis, and osteogenic differentiation of human mesenchymal stromal cells. J Proteome Res 12:378–389.

Krum SA, Chang J, Miranda-Carboni G, Wang CY. 2010. Novel function for NFκB: Inhibition of bone formation. Nat Rev Rheumatol 6:607–611.

Kunze R, Hempel U, Dieter P. 2010. Differential effect of chondroitin-4-sulfate on the immediate and delayed prostaglandin E(2) release from osteoblasts. Prostaglandins Other Lipid Mediat 92:8–12.

Lin F-H, Chang JB, McGuire MH, Yee JA, Brigman BE. 2010. Biphasic effects of interleukin-1β on osteoblast differentiation in vitro. J Orthopaedic Res 28:958–964.

Macri L, Silverstein D, Clark R. 2007. Growth factor binding to the pericellular matrix and its importance in tissue engineering. Adv Drug Deliv Rev 59:1366–1381.

Magnani A, Albanese A, Lamponi S, Barbucci R. 1996. Blood-interaction performance of differently sulphated hyaluronic acids. Thromb Res 81:383–395.

Magnani A, Lamponi S, Rappuoli R, Barbucci R. 1998. Sulphated hyaluronic acids: A chemical and biological characterisation. Polym Int 46:225–240.

Martell-Pelletier J, Kwan Tat S, Pelletier J-P. 2010. Effects of chondroitin sulfate in the pathophysiology of osteoarthritic joint: a narrative review. Osteoarthritis Cartilage 18:S7–S11.

Mumme M, Scotti C, Papadimitripopoulos A, Todorov A, Hoffmann W, Bocelli-Tyndall C, Jakob M, Wendt D, Martin I, Barbero A. 2012. Interleukin-1β modulates endochondral ossification by human adult bone marrow stromal cells. Eur Cells Mater 24:224–236.

Nagahata M, Tsuchiya T, Ishiguro T, Matsuda N, Nakatsuchi Y, Teramoto A, Hachimori A, Abe K. 2004. A novel function of N-cadherin and Connexin43: Marked enhancement of alkaline phosphatase activity in rat calvarial osteoblast exposed to sulfated hyaluronan. Biochem Biophys Res Commun 315:603–611.

Nakao S, Ogata Y, Shimizu E, Yamazaki M, Furuyama S, Sugiya H. 2002. Tumor necrosis factor alpha (TNF-alpha)-induced prostaglandin E2 release is mediated by the activation of cyclooxygenase-2 (COX-2) transcription via NFkappaB in human gingival fibroblasts. Mol Cell Biochem 238:11–18.

Novack DV. 2011. Role of NF-κB in the skeleton. Cell Res 21:169–182.

Oeckinghaus A, Hayden MS, Ghosh S. 2011. Crosstalk in NF-κB signaling pathways. Nat Immunol 12:695–708.

Oswald J, Boxberger S, Jùrgensen B, Feldmann S, Ehninger G, Bornhäuser M, Werner C. 2004. Mesenchymal stem cells can be differentiated into endothelial cells in vitro. Stem Cells 22:377–384.

Pecchi E, Priam S, Mladenovic Z, Gosset M, Saurel A-S, Aguilar L, Berenbaum F, Jacques C. 2012. A potential role of chondroitin sulfate on bone in

osteoarthritis: inhibition of prostaglandin E2 and matrix metalloproteinases synthesis in interleukin-1β-stimulated osteoblasts. Osteoarthritis Cartilage 20:1727–1135.

Perkins ND. 2006. Post-translational modifications regulating the activity and function of the nuclear factor kappa B pathway. Oncogene 25:6717–6730.

Pietrogrande L, Raimondo E, Fossali A, Taolino C. 2011. Biological and pharmacological factors influencing the fracture healing. Aging Clin Exp Res 2(Suppl):65–68.

Pittenger MF. 2008. Mesenchymal stem cells from adult bone marrow. Methods Mol Biol 449:27–44.

Redlich K, Smolen JS. 2012. Inflammatory bone loss: Pathogenesis and therapeutic intervention. Nat Rev Drug Discov 11:234–250.

Salbach J, Kliemt S, Rauner M, Rachner TD, Goettsch C, Kalkhoff S, von Bergen M, Möller S, Schnabelrauch M, Hintze V, Scharnweber D, Hofbauer LC. 2012a. The effect of the degree of sulfation of glycosaminoglycans on osteoclast function and signaling pathways. Biomaterials 33:8418–8429.

Salbach J, Rachner TD, Rauner M, Hempel U, Anderegg U, Franz S, Simon JC, Hofbauer LC. 2012b. Regenerative potential of glycosaminoglycans for skin and bone. J Mol Med 90:625–635.

Scotti C, Piccinini E, Takizawa H, Todorov A, Bourgine P, Papadimitropoulos A, Barbero A, Manz MG, Martin I. 2013. Engineering of a functional bone organ trough endochondral ossification. PNAS 110:3997–4002.

Thomas MV, Puleo DA. 2011. Infection, inflammation, and bone regeneration: A paradoxical relationship. J Dent Res 90:1052–1061.

Tomchuck SL, Zwezdaryk KJ, Coffelt SB, Waterman RS, Danka ES, Scandurro AB. 2008. Toll-like receptors on human mesenchymal stem cells drive their migration and immunomodulating responses. Stem Cells 26:99–107.

Volpi N. 2011. Anti-inflammatory activity of chondroitin sulphate: New functions from an old natural macromolecule. Immunopharmacol 19:299–306.

Yang X, Ricciardi BF, Hernandez-Soria A, Shi Y, Pleshko Camacho N, Bostrom MP. 2007. Callus mineralization and maturation are delayed during fracture healing in interleukin-6 knockout mice. Bone 41:928–936.